ACS OMEGA

http://pubs.acs.org/journal/acsodf

Article

Preliminary Evaluation of *Lablab purpureus* Phytochemicals for Anti-BoHV-1 Activity Using In Vitro and In Silico Approaches

Smitha S. Bhat,[#] Sushma Pradeep,[#] Sharanagouda S. Patil, Norma Flores-Holguín, Daniel Glossman-Mitnik, Juan Frau, Sarana Rose Sommano, Nemat Ali, Mohamed Mohany, Chandan Shivamallu,* Shashanka K. Prasad,* and Shiva Prasad Kollur*

Cite This: *ACS Omega* 2023, 8, 22684−22697

Read Online

ACCESS | Metrics & More | Article Recommendations

ABSTRACT: *Lablab purpureus* from the Fabaceae family has been reported to have antiviral properties and used in traditional medical systems like ayurveda and Chinese medicine and has been employed to treat a variety of illnesses including cholera, food poisoning, diarrhea, and phlegmatic diseases. The bovine alphaherpesvirus-1 (BoHV-1) is notorious for causing significant harm to the veterinary and agriculture industries. The removal of the contagious BoHV-1 from host organs, particularly in those reservoir creatures, has required the use of antiviral drugs that target infected cells. This study developed LP-CuO NPs from methanolic crude extracts, and FTIR, SEM, and EDX analyses were used to confirm their formation. SEM analysis revealed that the LP-CuO NPs had a spherical shape with particle sizes between 22 and 30 nm. Energy-dispersive X-ray pattern analysis revealed the presence of only copper and oxide ions. By preventing viral cytopathic effects in the Madin−Darby bovine kidney cell line, the methanolic extract of *Lablab purpureus* and LP-CuO NPs demonstrated a remarkable dose-dependent anti-BoHV-1 action in vitro. Furthermore, molecular docking and molecular dynamics simulation studies of bio-actives from *Lablab purpureus* against the BoHV-1 viral envelope glycoprotein disclosed effective interactions between all phytochemicals and the protein, although kievitone was found to have the highest binding affinity, with the greatest number of interactions, which was also validated with molecular dynamics simulation studies. Understanding the chemical reactivity qualities of the four ligands was taken into consideration facilitated by the global and local descriptors, which aimed to predict the chemical reactivity descriptors of the studied molecules through the conceptual DFT methodology, which, along with ADMET finding, support the in vitro and in silico results.

INTRODUCTION

Bovine alphaherpesvirus 1 (BoHV-1), belonging to the α-Herpesviridae family, is one of the eight herpesviruses that are accountable for major economic damage in the cattle sector.[1] Three distinct subtypes of the virus are named BoHV-1.1, 1.2a, and 1.2b.[2] The genital variants of the virus are reported with an incubation period of 2−6 days exhibiting clinical signs such as recurrent micturition and minor genital infection.[3] Swollen vulvae, tiny papules, and ulcers on mucosal surfaces, with comparable lesions on bulls, are also commonly documented in infected cattle. Secondary bacterial co-infections may be noted, with uterine inflammation, transitory sterility, and pus-filled vaginal discharge. The BoHV-1 infections are known for their notoriety across the cattle industry with reports of nearly a billion dollar losses in the United States alone.[4−6] Pourmahdi Borujeni et al. reported the seroprevalence of BoHV-1 to be 28.4%;[7] meanwhile, another study conducted by Lanave et al. concluded that as many as 26 out of 59 lactating cows are usually affected by an outbreak of bovine herpetic mammilitis.[8] In India, BoHV-1 was first isolated and characterized while investigating conjunctivitis in a herd from Uttar Pradesh,[9] and the overall prevalence was identified to be as high as 32.84%[10] in cattle with the reproductive disorder. Seroprevalence studies have found the BoHV-1 infection to be widespread across all Indian states.[11]

Although there are significant similarities in the pathogenic mechanism of BoHV-1 and human herpesviruses, the former is found to have a quicker replication cycle and the capability to inflict lifelong damage in the host.[12] Following an initial nasal and vaginal infection, latency is established in the sacral ganglia, which reactivate later during the lifetime of the animal.[13] The viral reactivation is regarded as a potential source of semen contamination as well.[14] Currently, BoHV-1 is

Received: March 5, 2023
Accepted: May 31, 2023
Published: June 14, 2023

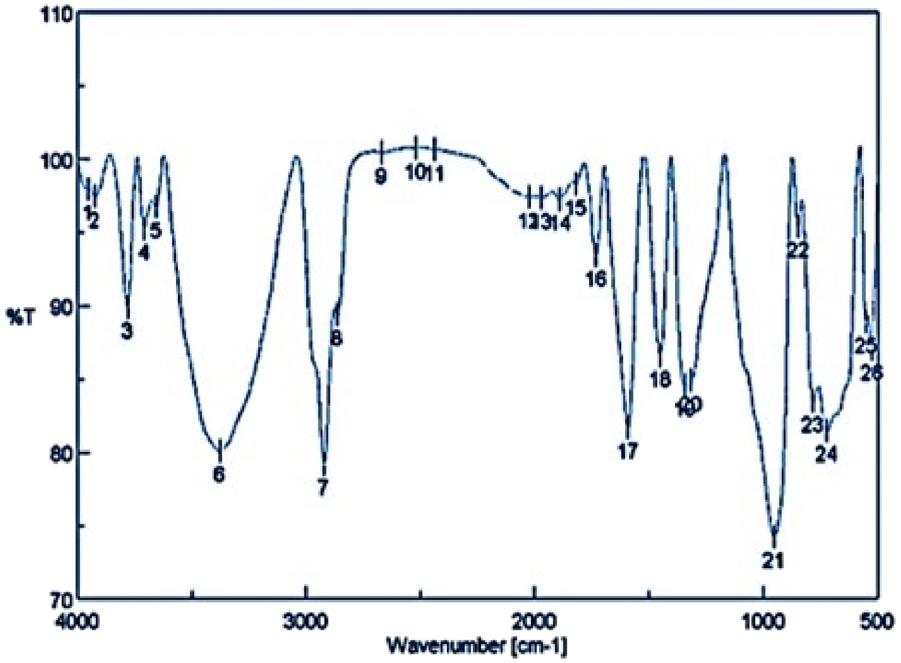

Figure 1. FTIR spectrum of as-prepared LP-CuO NPs showing significant stretching vibrations.

used as a disease model and substitute for herpesvirus infection control in both humans and animals.[15] Vaccination against BoHV-1 infection was observed to be effective in the severity control of clinical symptoms. Yet, prophylaxis has been reported to confer limited protection against the infection.[16] Furthermore, chemical antiviral medications reportedly have several drawbacks including toxicity and drug resistance development, implying the need for novel, nontoxic antiviral drugs with target-specific activity to reduce the viral load on host organs and in reservoir animals.[17,18] Crude aqueous extracts of leaves of *Bumelia sertorum*, *Coffea arabica*, *Endopleura uchi*, *Leandra purpurensis*, *Prunus myrtifolia*, *Psidium cattleyanum*, *Symphyopappus compresses*, and *Uncaria tomentosa* displayed anti-BoHV-1 activity; however, the mechanism of action of these extracts remain unidentified.[19] *Peumus boldus* also presented activity against BoHV-1 with 99% of inhibition.[20] Leaf extracts of *Artocarpus heterophyllus* demonstrated an in vitro anti-herpesvirus effect.[21] Curcumin has been confirmed to have antiviral activity against BoHV-1 by impacting the lipid raft formation.[22]

Numerous researchers have established the role of plants and their phytoconstituents in the prevention of viral entry, multiplication, and release as well as their immune-boosting nature.[23−27] Although in vitro and in vivo experiments have been traditionally used for drug discovery in the past, drug failure has been seen in the majority of situations (40−60%) due to an absence of appropriate pharmacokinetic features on absorption, distribution, metabolism, excretion, and toxicity (ADME/Tox),[28] and they are time-consuming, expensive, and inaccurate. Clinical trial success is only 13% despite the substantial financial and time commitments needed for medication development, and there is a high drug attrition rate.[29] With the advent of bioinformatics, chemical informatics, and omics,[30,31] in silico techniques or computer-aided therapeutic target identification techniques have been gaining prominence as they intensely minimize the range of experimental targets, shorten the drug discovery and development cycle, and lower the experimental cost by combining big data with computational approaches. Leading pharmaceutical companies and researchers have accelerated the drug discovery and development process by using computer-aided drug discovery tools in early studies and lowering costs and failure rates in the latter stage.[32] Researchers can gain a better understanding of the molecular interactions and binding affinities between the target protein and plant compounds by utilizing CADD. In light of the recent coronavirus pandemic, several phytocompounds have also been evaluated for their anti-SARS-CoV-2 activity by in silico approaches.[33−40] Many researchers have explained the biological results of various experiments including anticancer and antiviral effects by molecular docking studies, which aid in a better understanding of the mechanism involved.[36,41−45] Natural compounds have also been found to effectively bind to the surface glycoprotein of the herpesvirus via virtual screening. Researchers have also identified potential drug targets in bovine herpesvirus 4 using computational techniques.[46]

Lablab purpureus (*LP*), from the Fabaceae family, is considered one of the most domesticated species of legumes and has recently gained popularity owing to its versatile, multifunctional biomedical properties. The plant bioactives have been widely used in traditional medicinal practices such as ayurveda and Chinese medicine to treat a range of ailments such as cholera, food poisoning, uterine inflammation, diarrhea, and phlegmatic disorders.[47] However, *LP* remains underutilized owing to its unpopularity, as compared to the other legumes, presumably due to its antinutritional factors and unappetizing nature. Nevertheless, the *LP* phytochemicals have now garnered scientific interest and are being researched concerning their potential biomedical properties including but not limited to antioxidant, anti-inflammatory, anticancer, antiviral, antifungal, and antibacterial effects.[48−57] In silico and in vitro investigations have reported dolichin, an antifungal chitinase-like compound, to be efficient in the inhibition of the human immunodeficiency virus-1 (HIV-1) by acting on the reverse transcriptase and glucosidase enzymes.[58,59] Luteolin has been observed to inhibit the in vitro viral entry and the

https://doi.org/10.1021/acsomega.3c01478
ACS Omega 2023, 8, 22684−22697

action of neuraminidase enzyme in influenza (Influenza virus A/Fort Monmouth/1/1947 (H1N1)).[60] The lablab agglutinin known as Flt3 receptor-interacting lectin (FRIL), a mannose-binding macromolecule, was found to possess the ability to bind to the human immunodeficiency viral (HIV) glycoprotein and promote the formation of the viral syncytium, resulting in the reduction of the viral load.[61] The ubiquity of *LP* plant phytochemicals and their potential utility in antiviral treatment is quite evident. Notwithstanding, there is a need for a better understanding of the mechanistic basis of the antiviral potential of *LP* phytochemicals.

Drug delivery via nanocarriers aids to overcome numerous challenges accompanying the traditional system of antiviral drug administration.[62−64] Green-synthesized metal/metal oxide nanoparticles (NPs), such as copper/copper oxide and silver/silver oxide NPs, prepared using phytocompounds, have gained popularity in recent years. Such NPs are usually less harmful, generally regarded as safe (GRAS), than their synthetic cousins, and are found to have an extensive range of medical applications alongside growing academic interests. A potential antiviral strategy currently under investigation is the discovery of efficient green-synthesized NP drug delivery systems that exploit viral access into cells via diverse cell-membrane receptors.[65]

While *LP* has been reported to possess an antiviral significance, there are very few studies conducted on NPs. In similar studies, green-synthesized zinc NPs have been reported to inhibit BoHV-1 infection in vitro.[65] Both zinc and silver NPs of crude olive leaf extracts, as well as honey, demonstrated minimal cytotoxicity and capacity to control or inhibit the bovine alpha herpesvirus in vivo in the rabbit model.[66] Although green-synthesized NPs have attracted great attention in the last decade, there is a lack of studies concerning the biological activity of green-synthesized copper oxide NPs of *LP*. Investigations focused on understanding the mechanism of their antiviral activity against latent BoHV-1 to identify highly effective drugs and delivery systems are critical. The novelty of the current study is that it investigates and compares, for the first time, the antiviral activity of *LP* methanol extracts and green-synthesized copper oxide NPs against BoHV-1, followed by molecular docking studies of reported phytochemicals against BoHV-1 proteins to identify the potential antiviral agents.

RESULTS

FTIR Analysis. The formation of as-prepared LP-CuO NPs was confirmed by infrared spectroscopy (Figure 1). Significant IR stretching bands were observed in the IR spectrum. The stretching band noticed at 568 cm^{-1} (band number 25 in Figure 2) was credited to the distinctive narrow and sharp stretching vibrations of CuO, which revealed the presence of CuO in the prepared sample. It is noteworthy to mention that the absorption bands noticed between 1642 and 1376 cm^{-1} were ascribed to the aromatic unsaturation (C═C) of the plant material. Moreover, an intense band at 964 cm^{-1} was detected, due to C−O stretching from phytochemicals. Furthermore, the presence of a broad band around 3453 cm^{-1} was the distinctive absorption for O−H−O of water and −OH stretching of ethanolic species.

SEM Analysis. The surface morphology of the obtained LP-CuO NPs was investigated by SEM analysis (Figure 2). It is evident from the SEM image that the mean particle size of the as-obtained LP-CuO NPs was about 22−30 nm with a spherical shape and they have good homogeneity and appropriate separation. However, a small amount of agglomeration was observed, which may be owed to the formation of aggregation.

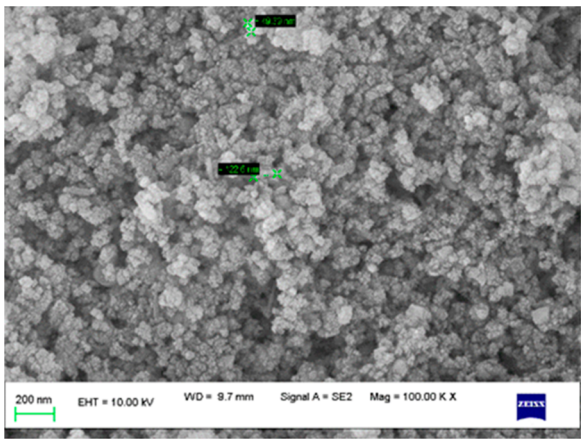

Figure 2. SEM image of LP methanolic seed extract-derived LP-CuO NPs.

EDX Analysis. Figure 3 depicts the energy-dispersive X-ray pattern, aiding in the assessment of elemental composition (i.e., oxygen 34.67% and copper 65.33% by mass) of the as-prepared LP-CuO NPs. The outcomes from EDX analysis established that copper and oxide were the only ions existing in the as-prepared material with the equal ratio as demarcated at the period of experimentation.

Cytotoxicity Assay. The cytotoxicity of LP-CuO NPs and the *LP* extract on MDBK cell lines was evaluated with the crystal violet assay. Results of the toxicity assay on MDBK cells indicated that among the tested samples, the least toxicity was found in the *LP* extract with a maximum nontoxic concentration (MNTC) of 1200 μg/mL, whereas LP-CuO NPs showed slightly higher toxicity with MNTC 800 μg/mL (Figure 4).

Viruses were treated with test samples in multiple dilutions lower than the MNTC.

Inhibition of CPE was observed in 25, 50, 100, 250, 500, and 750 μg/mL concentrations of *LP* extracts, LP-CuO NPs, and CuO NPs observed after 48 h of treatment. The antiviral activity of the *LP* extract, CuO NPs, and LP-CuO NPs against BoHV-1 CPE showed a substantial reduction (p-value <0.05) (Figure 5). The outcome of the assay is presented as the percentage of plaque inhibition from mean values from triplicate experiments. 79.8% plaque inhibition was induced at concentrations of 750 μg/mL of the *LP* extract, while 87.4% inhibition was observed due to CuO NPs at the same concentration, whereas LP-CuO NPs showed 100% plaque inhibition at 750 μL/mL and 99% inhibition at 500 μL/mL with 42.7% inhibition at 50 μg/mL.

The graph represents a substantial reduction in viral CPE in all treatment groups. Concentration- and time-dependent inhibition of BoHV-1 could be demonstrated by these test samples. In comparison, the cells treated with LP-CuO NPs showed the highest efficiency against viral load.

Molecular Docking Studies. Assessment of the binding mode and steadiness of the ligand with bovine herpesvirus 1 glycoprotein D (PDB ID: 6LSA) was accomplished using the PyRx module of AutoDock Vina. The binding conformation of ligands was investigated using docking analysis. The binding

https://doi.org/10.1021/acsomega.3c01478
ACS Omega 2023, 8, 22684−22697

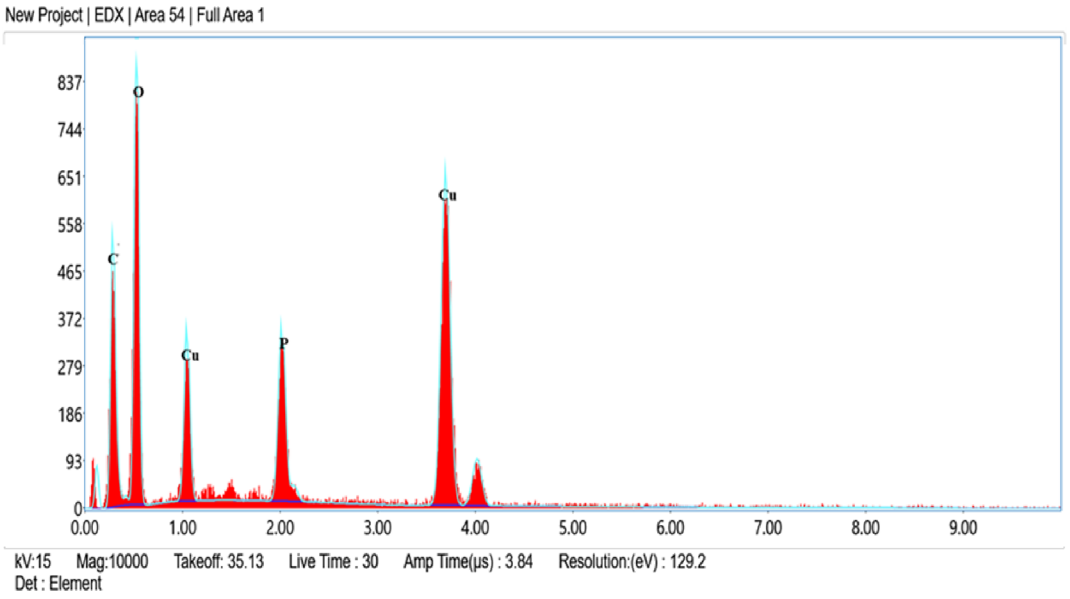

Figure 3. EDX spectrum of the as-prepared LP-CuO NPs.

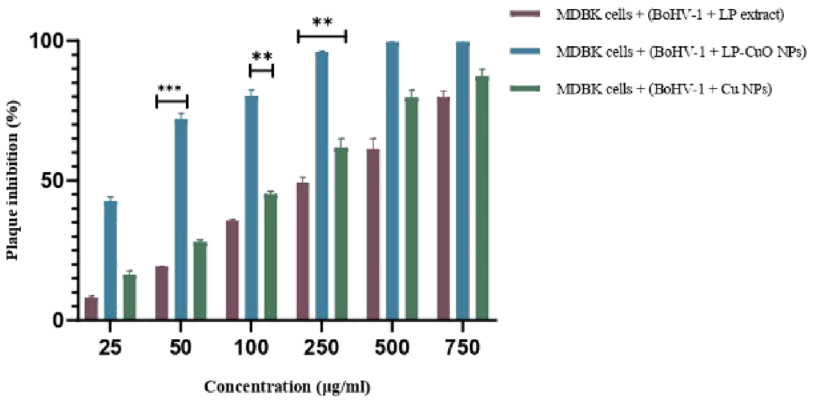

Figure 4. Plaque inhibition on MDBK cell lines. Data signifies mean ± SEM (n = 3).

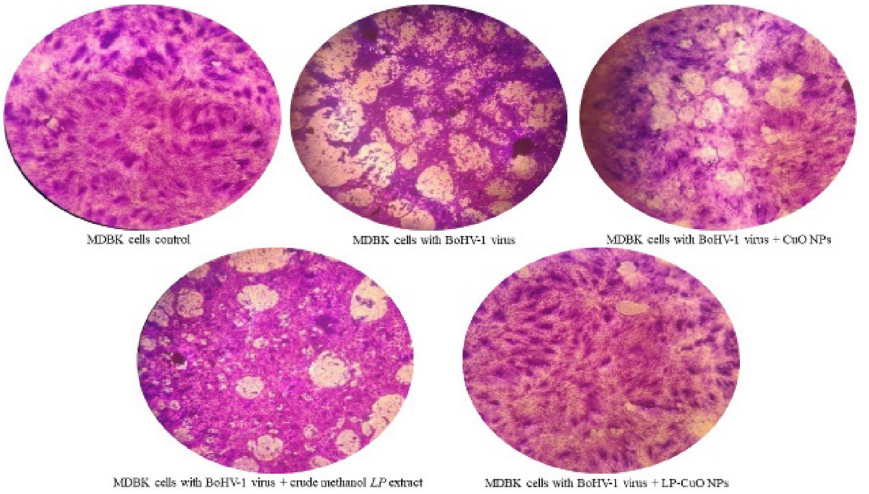

Figure 5. Inhibition of cytopathic effects on MDBK cell lines.

conformation of the chemical(s) to the protein was discovered, and the conformation with the lowest binding energy was obtained. In comparison to higher energy values, lower energy scores demonstrated a better protein-ligand binding affinity. Compared to the standard drug dexamethasone, the ligand kievitone had the highest affinity (−8.9 kcal/mol), with the greatest number of interactions (4) with 6LSA, of all the four selected molecules (Figure 6A−E).

Molecular Dynamics Simulations. Based on the results of docking, we selected glycoprotein for molecular dynamics

https://doi.org/10.1021/acsomega.3c01478
ACS Omega 2023, 8, 22684−22697

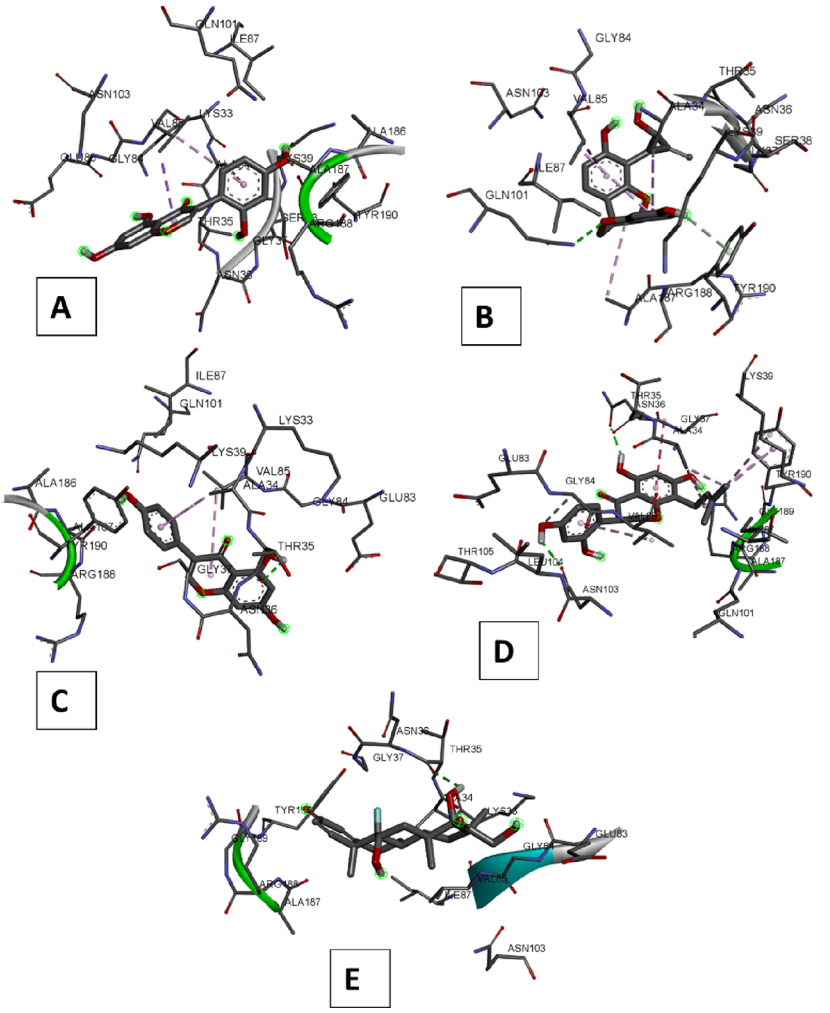

Figure 6. The detailed representation of 3D interactions obtained between the protein 6LS9 with respective ligands. (A) Dolichin A, (B) luteolin, (C) 2-hydroxygenistein, (D) kievitone, and (E) brassinolide.

simulation. The simulation was carried out on the glycoprotein-unbound system as well as on systems bound to kievitone and dexamethasone, in order to study the dynamic behavior of the protein. We also performed simulations on the glycoprotein bound with its experimentally validated inhibitor for comparison. Quality checks were performed on the simulated systems to ensure their validity, and the results showed that the parameters were stable throughout the simulation period. The simulations did not result in any significant alterations in the density, temperature, volume, kinetic/potential/total energies, and pressure of the unbound and lead ligand/standard inhibitor−bound protein/protein complex during the 20 ns simulation period. The RMSD and RMSF of the complexes did not show any significant deviation in comparison to the unbound protein, except for a significant reduction in RMSF values in the Kievitone-bound glycoprotein complex. Solvent-accessible surface area analysis showed that Kievitone binding did not affect the SASA value significantly in comparison to the standard drug. Hydrogen bond formation analysis showed that kievitone binding favored H-bond formation in comparison to dexamethasone binding to the glycoprotein during the simulation period. The results are presented in Figure 7.

Conceptual DFT Studies. Table 1 presents the computed global reactivity descriptors, calculated using the approach described below together with the custom CDFT software tool.[67−72]

It can be inferred that brassinolide was the least reactive of the ligands, followed by dolichin A and kievitone, with 2′-hydroxygenistein and luteolin being the most reactive ligands, taking into consideration the global hardness η, which is considered as a thorough quantity of the electron density deformation and chemical reactivity due to the HOMO−LUMO gap. The electron-donating capacity $\omega-$ is considered an added imperative measure for ligands as compared to their electron-accepting power $\omega+$. A comparison of both these factors for each molecule found the highest electron-donating power in luteolin followed by 2′-hydroxygenistein, kievitone, and with the lower values for brassinolide and dolichin A. The balance between the resistance of a particle against switching electron density with the environment and an electrophile's propensity to attain additional electron density is represented by the electrophilicity index (ω).[73]

By comparing the electrophilicities of a number of substances employed in Diels−Alder processes, an electrophilicity measure for identifying organic molecules as ranging from strong to marginal was theorized as follows: $\omega > 1.5$ eV for the first, $0.8 < \omega < 1.5$ eV for the second, and $\omega < 0.8$ eV for the final instance.[74−76] Thereby, except for brassinolide and dolichin, Table 2 suggests that all other selected ligands may be

https://doi.org/10.1021/acsomega.3c01478
ACS Omega 2023, 8, 22684−22697

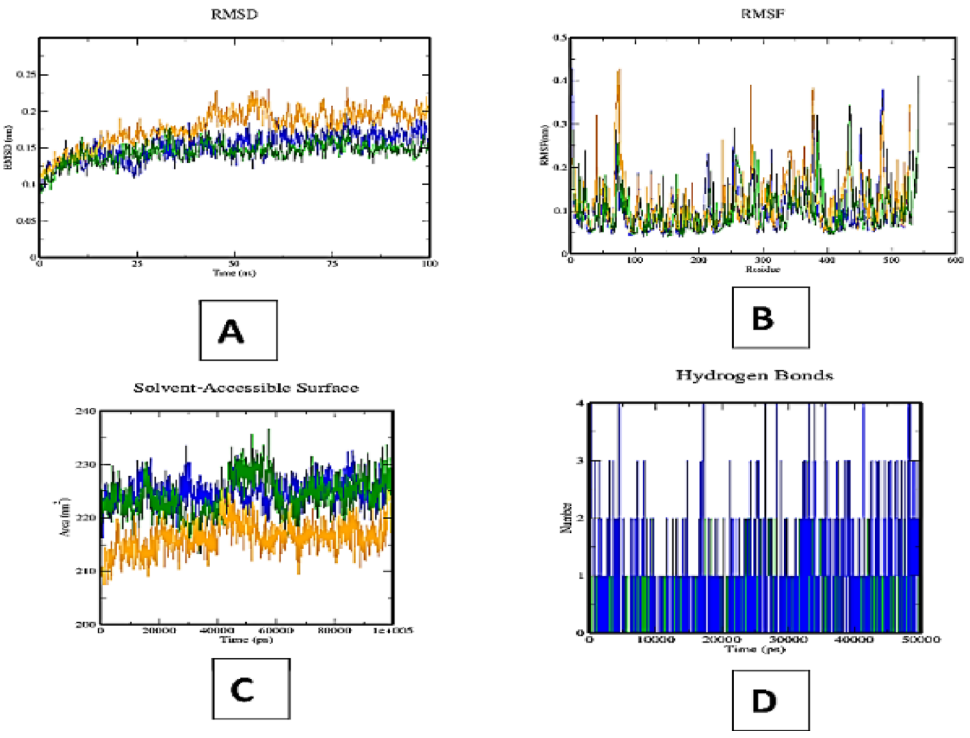

Figure 7. Molecular dynamics simulation. (A) RMSD, (B) RMSF, (C) SASA, and (D) hydrogen bond plots of kievitone (blue) and dexamethasone (orange) bound to glycoprotein 6LSA (green).

Table 1. Predicted Global Chemical Reactivity Descriptors for the Ligands Selected (All but S in eV, S in eV^{-1})

molecule	χ	η	ω	S	N	ω^-	ω^+	$\Delta\omega^{\pm}$
brassinolide	3.6991	6.3441	1.0784	0.1576	1.9214	4.4030	0.7038	5.1068
dolichin A	3.3175	4.9489	1.1119	0.2021	3.0006	4.1919	0.8744	5.0663
2′-hydroxygenistein	3.8880	3.7492	2.0159	0.2667	3.0299	6.2102	2.3222	8.5324
kievitone	3.8184	4.3127	1.6904	0.2319	2.8177	5.5596	1.7411	7.3007
luteolin	4.1918	3.7277	2.3568	0.2683	2.8369	7.0425	2.8507	9.8933

Table 2. Interaction Details of All Six Ligands with the 6LS9 Protein

sl no.	ligand name	binding energy (kcal/mol)	hydrogen bond forming amino acid residues
1	dolichin A	−7.3	GLY-115, TYR-24, LYS-222, ASP-138
2	luteolin	−8.1	ASP-138, PRO-238, TYR-239
3	2-hydroxygenistein	−7.6	TYR-239, ASP-137, PRO-238
4	**kievitone**	**−8.2**	**PRO-237, THR-136, ASP-138, ARG-157**
5	brassinolide	−7.2	ASP-138, PRO-238, LYS-222

potent electrophiles. Local analogs of the global reactivity descriptors have also been developed to comprehend the alterations in chemical reactivity between the atoms in the molecule. The Fukui functions and the dual descriptor, which relate to the electronic densities of the neutral, positive, and negative species, are among these local reactivity descriptors defined as nucleophilic Fukui function (NFF) = $\rho N + 1(r) - \rho N(r)$, electrophilic Fukui function (EFF) = $\rho N(r) - \rho N - 1(r)$, and dual descriptor (DD) = $(\partial f(r)/\partial N)\upsilon(r)$, relating to the electronic densities of the neutral, positive and negative species.[77−86]

NFF stands for nucleophilic attack-prone molecular system sites, whereas EFF stands for electrophilic attack-prone molecular system sites. Although it has been demonstrated that the DD can clearly distinguish between nucleophilic and electrophilic sites, both the NFF and the EFF have been successfully used to identify reactive regions.[84−86] Figure 8 depicts graphical representations of the DD.

The sections on the ligands where DD deviates from 0 reflect chemical reactivity variances and may be distinguished using a graphical representation even though there is considerable overlap between the various locations within the ligands.

Computational Pharmacokinetics Report. Table 3 lists the bioactivity scores for the five ligands, which are indicators of how well the molecules behave or engage with various receptors.

While a molecular structure with a bioactivity score ranging from −0.50 to 0.00 is expected to have moderate biomedical activity, one with a value of more than 0 is most likely to exhibit strong biological activities. If the bioactivity score is less than −0.50, the molecular system is considered inactive. The intriguing findings from Table 3 demonstrate that, except for dolichin A, all five ligands were found to behave as kinase and enzyme inhibitors.

The ADMET study evaluates the pharmacokinetics of a medicine. Predicting a drug's fate and its properties on the

https://doi.org/10.1021/acsomega.3c01478
ACS Omega 2023, 8, 22684−22697

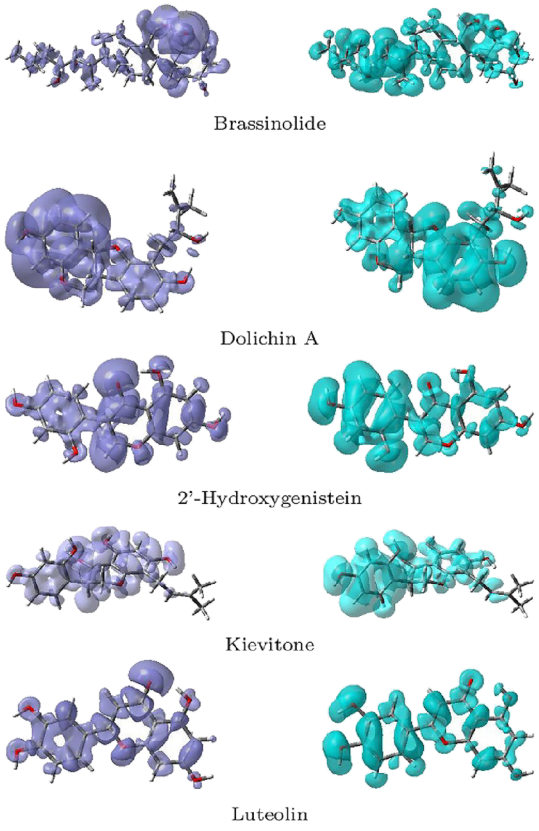

Figure 8. Dual descriptor of the selected ligands. Left: DD > 0, right: DD < 0.

body, such as the amount of a medication consumed orally and the amount that is retained within the gastric system, is a crucial fragment of the medication development process. Inadequate absorption could cause nephrotoxicity and neurotoxicity, much like how it would affect distribution and metabolism. Understanding the reactivity of a drug molecule inside a living entity is the aim of this study. The ADMET analysis is thus one of the vital elements of in silico design. The calculated ADMET pharmacokinetic profile of the selected ligands is represented in Table 4.

Interesting results can be seen in the computed ADMET profiles of the ligands predicted employing the pkCSM platform, with brassinolide and luteolin showing higher intestine absorption than the other ligands. Additionally, all the ligands are possible substrates for cytochrome P-450 isoforms. Only brassinolide, in contrast to the other ligands, has the potential to be a P-gp I inhibitor, meaning that none of the other ligands will operate as P-gp II inhibitors. The fact that none of the ligands will be hERG I inhibitors while dolichin A, 2′-hydroxygenistein, and luteolin may be hERG II inhibitors is intriguing. The central nervous system penetrability of these compounds was exceedingly poor, as indicated by the predicted values of logBB and logPS.

DISCUSSION

Historically, therapeutic plants have been used to treat an assortment of illnesses, including communicable ailments that affect both humans and animals. As much as 70−80% of the globe's populace is reported to be using herbal remedies.[87] Utilization of herbal plants and their extracts to promote healing, raise energy, reduce symptoms, support the immune system, and lengthen and improve the quality of animal lives presented a new chance to elevate the practice of veterinary medicine.[88] Some researchers propose that the reason for in vitro viral inactivation may be due to the protein coat being preferentially bound by the polyphenols. Tannins and alkaloids have also been reported to have antiviral properties.[89,90] The greatest economic losses are caused by abortions resulting in a significant loss of economic and valuable genetic potential.[88] Acyclovir, famciclovir, and fenbendazole are common examples of traditional synthetic medications that have been reported to have inhibitory effects against BoHV-1 when taken alone or in conjunction with natural products.[91] The probable antiviral activity of a fungal secondary metabolite, 3-*O*-methylfunicone produced by *Talaromyces pinophilus*, has been reported.[92] In addition to inhibiting BoHV-1, *Guazuma ulmifolia* and *S. adstringens* also prevented the production of viral proteins in cell cultures.[93] Various plants *Azadirachta indica, Pteris vittata, Mitragyna parvifolia*, and *Ocimum sanctum* have been observed to contain powerful inhibitors of the BoHV-1 virus, providing nearly 85% defense against it.[88]

One of the most difficult tasks facing medical science is the creation of antiviral medicines. CuO NPs display unique properties and could function as a cutting-edge treatment for viral infection. Metal NPs' antiviral properties have drawn a lot of research interest in recent times. Notwithstanding, the exact mechanism behind their activity is still unknown. When used as antimicrobial agents, metal NPs like silver and gold NPs have garnered a lot of interest due to their effective repressive action against a variety of viruses.[94,95] Metal NPs may interact with viral surfaces, interfere with viral attachment, prevent viruses from entering cells, interact with viral genomes, prevent viruses from replicating, inhibit protein synthesis, and prevent viruses from assembling and releasing virions as potential mechanisms for their antiviral activity.[94,95] Contrary to other metals, copper is a trace metal that is vital to human health and is important to the functioning of all living things.[96] Copper is thought to be harmless for people, as established by the use of copper intrauterine devices extensively for a long time in gynecology.[97]

The maximal nontoxic concentrations of both the crude methanol extracts, CuO NPs, and the LP-CuO NPs were examined in the MDBK cell line. BoHV-1's cytotoxic effect was

Table 3. Predicted Bioactivity Scores for the Five Studied Ligands

property	brassinolide	dolichin A	2′-hydroxy genistein	kievitone	luteolin
GPCR ligand	0.20	0.39	−0.18	0.09	−0.02
ion channel modulator	0.08	0.08	−0.53	0.04	−0.07
protease inhibitor	0.28	0.03	−0.64	−0.05	−0.22
nuclear receptor ligand	−0.28	−0.04	−0.04	0.00	0.26
kinase inhibitor	0.57	0.75	0.29	0.69	0.39
enzyme inhibitor	0.48	0.71	0.08	0.48	0.28

https://doi.org/10.1021/acsomega.3c01478
ACS Omega 2023, 8, 22684−22697

Table 4. Computed ADMET Pharmacokinetic Profile of the Five Studied Ligands

property	model	brassinolide	dolichin A	2'-hydroxy genistein	kievitone	luteolin
absorption	HIA	79	94	77	75	84
	P-gp substrate	+	+	+	+	+
	P-gp I inhibitor	+	-	-	-	-
	P-gp II inhibitor	-	-	-	-	-
distribution	logBB	-0.89	-0.80	-1.14	-1.15	-1.15
	logPS	-2.49	-2.31	-2.36	-3.13	-2.47
metabolism	CYP2D6 substrate	-	-	-	-	-
	CYP3A4 substrate	+	-	-	-	-
	CYP1A2 inhibitor	-	+	+	+	+
	CYP2C19 inhibitor	-	+	-	+	-
	CYP2C9 inhibitor	-	+	-	-	-
	CYP2D6 inhibitor	-	-	-	-	-
	CYP3A4 inhibitor	-	+	-	-	+
excretion	OCT2 substrate	-	-	-	-	-
toxicity	AMES toxicity	-	+	+	+	-
	hERG I inhibitor	-	-	-	-	-
	hERG II inhibitor	-	+	+	-	+

demonstrated by the rounding and ballooning of the cells, as well as by the formation of clusters of spherical cells occurring in a grape-like arrangement, around the opening of the cell line monolayer. The maximal nontoxic concentration was determined to be the dose at which no degenerative changes in the cell culture were seen. Since their greater concentrations were unable to cause toxicity in the cells, both the extract and LP-CuO NPs appeared to be quite safe for in vivo research. Compared to the *LP* extract and CuO NPs, LP-CuO NPs showed a greater reduction in the viral cytopathic effects ($P < 0.05$). Hence, our findings suggest that LP-CuO NPs displayed a substantial repressive effect on the action of BoHV-1 at a non-cytotoxic concentration, demonstrating their potential as antiviral therapeutics.

Bovine herpesvirus 1 (BHV-1) has similar biological properties to HSV-1, is essential for virus-induced cell fusion and efficient virus entry, and is an important health concern to the livestock industry.[98] BoHV-1 surface glycoproteins have a part in the virus's capacity to adhere to cell membranes and fuse with them. Nectin-1, herpesvirus entry mediator, and 3-*O*-sulfated heparan sulfate (3-OS HS) are three biological receptors that the BoHV-1 glycoprotein gD interacts with.[99] The virus attaches to the cell and merges with the cell membrane as a result of the gD protein's interaction with the receptors. This protein can be utilized as a target protein to look for medicines that prevent HSV-1 infection in its early stages. The second goal of this study was to learn more about how phytocompounds of *LP* with antiviral capabilities can effectively inhibit the BoHV-1 through in silico studies. In silico approaches based on bioinformatics tools and software have sped up the development of new drugs to block important viral proteins and treat viral infections. The envelope glycoprotein of BoHV-1 was used as the target protein in this work, and five phytocompounds, luteolin, brassinolide, dolichin A, kievitone, and 2-hydroxygenistein, previously identified in *LP* with antiviral and anti-inflammatory activities, were docked to determine the binding mode with the lowest binding energy. Interestingly, kievitone demonstrated an extraordinarily high binding affinity toward the target protein. It was shown with molecular docking that the ligands can block BoHV-1 infection by directly networking with the viral gD protein and interfering with virus adsorption. Molecular dynamic simulations also demonstrated that kievitone binding favored H-bond formation in comparison to standard drug binding to the glycoprotein during the entire simulation period.

In the current scenario, several studies have indicated hundreds of phytochemicals as potential inhibitors of BoHV-1 target proteins. However, most of the studies do not identify or predict a single phytochemical as an inhibitor. Prediction of common inhibitor potential drugs could reduce a lot of time and wealth in the course of finding a suitable phytotherapeutic compound. Therefore, our study stands exceptional in the class of similar studies.

CONCLUSIONS

The outcomes of the current study proved the dose-dependent antiviral activity of crude methanolic *LP* seed extracts and their copper oxide NPs against BoHV-1 in vitro. Furthermore, to prove the findings obtained from antiviral activity, in silico molecular docking interaction studies were conducted to ascertain the efficiency of the LP phytochemicals against the envelope glycoprotein of the BoHV-1 virus. The ligand kievitone exhibited the lowest binding energy and highest binding affinity toward the selected protein, thus supporting the in vitro findings and confirming the presence of a potent anti-BoHV-1 agent in *LP*.

The DFT calculations aimed to predict the chemical reactivity descriptors of the studied molecules through the conceptual DFT methodology support the in vitro and in silico results. Thus, all this information implies the need for further in vivo validation, isolation, and identification of bioactive molecules responsible for the observed antiviral activity of *Lablab purpureus* phytochemicals to be developed into potent antiviral agents for veterinarian therapeutic applications.

MATERIALS AND METHODS

Seed Procurement and Extraction. Fresh seeds of *LP* were collected from Hunsur district, Karnataka, India, authenticated at the Indian Institute of Horticultural Research, cleaned under tap water, and dried in shade. The seeds were then powdered using a blender and subjected to Soxhlet extraction according to Prasad et al. for 4 h at 60 °C.[100] Experimentally, 20 g of powdered seeds bound in muslin cloth

https://doi.org/10.1021/acsomega.3c01478
ACS Omega 2023, 8, 22684−22697

was placed in the thimble and phytochemicals were extracted using 200 mL of 99% methanol as a solvent. The resultant suspension collected in the round-bottom flask was cooled, filtered, and Rota-evaporated to obtain dry extracts. The extract yield was recorded and stored in an air-tight container at −20 °C.

Green Synthesis of LP Phytochemical-Infused Copper Oxide Nanoparticles (LP-CuO NPs). LP-CuO NPs were prepared by mixing 0.5 g of prepared *LP* seed methanolic extract dissolved in 5 mL of methanol and 45 mL of 10 mM copper sulfate dehydrate solution with constant magnetic stirring at 60 °C for 6 h. The blue-colored solution turned green over a period of 4 h, and finally, a dark-brown precipitate was collected upon centrifugation. The sediment was carefully collected, washed with distilled water, and air-dried. Furthermore, to confirm the presence of NPs, the air-dried sediment was subjected to characterization.[101]

Cell Culture. The cell culture was carried out according to Ansari et al.,[102] wherein 2×10^5 cells of the Madin−Darby bovine kidney (MDBK) cell line were cultivated in minimum essential medium (MEM) with antibacteria, 100 units/mL of penicillin, and 100 μg/mL of streptomycin and incubated at 37 °C in the presence of carbon dioxide (5%).

Cytotoxicity Assay. Evaluation of cytotoxicity of the methanolic *LP* seed extract and CuO NPs and LP-CuO NPs was performed by the crystal violet method according to Feoktistova et al.[103] The experiment was conducted in a 96-well plate. The MDBK cells were seeded for 24 h at 37 °C with 5% CO_2 to enable the adhesion of cells to wells, following which the culture medium was recanted. For determining the MNTC for the antiviral assay, the cells were then added with 100 μL of fresh MEM (Merck), with Earle's salts and L-glutamine, without sodium bicarbonate, supplemented with different concentrations of LP-CuO NPs (ranging from 5 to 1200 μg/mL) and incubated for 48 h in triplicates.

After incubation, the contents of the well were aspirated and the washing procedure was repeated and then stained with 50 μL of 1% solution of crystal violet and incubated for 20 min. The crystal violet was then removed, and wells were washed and air dried. Following this, 200 μL of methanol was added to each well and set aside for 20 min, following which the absorbance was measured at 570 nm.

A similar procedure was repeated using different concentrations of *LP* extracts (ranging from 5 to 1200 μg/mL) and CuO NPs (not bound to the plant material, ranging from 5 to 1200 μg/mL) for evaluation of their cytotoxicity. MDBK cells free of the sterile NPs of *LP* seed extracts were used as controls. 100% viability was allocated to the mean absorbance of the control cells.

Antiviral Assay. The antiviral potency of *LP* seed methanolic extracts, CuO NPs, and LP-CuO NPs was evaluated by determination of inhibition of plaque formation according to Ansari et al.[102] Monolayers of MDBK cells were subjected to infection with the BoHV-1 (2×10^5 PFU/cell) and incubated at room temperature. Varied concentrations (at least five dilutions less than MNTC) of the test samples (LP-CuO NPs, *LP* extracts, and CuO NPs) were added to these wells and incubated for 2 days at 37 °C. The medium was then aspirated, and the wells were rinsed with sterile phosphate-buffered saline. 500 μL of methanol was added to each of the wells and re-aspirated after 15 min. These cells were then fixed with formalin (10%) prior to being subjected to staining with 200 μL of 1% solution of crystal violet for 45 min. The stained cells were washed, and the plaques were then observed under the microscope. Calculation of the percentage of reduction in plaque was relative to the amount of plaque formation in the absence of the tested compounds. Virus-infected cells were left untreated to be used as control.

Library and Macromolecule Preparation. The structure of the envelope glycoprotein was obtained in PDB format from the PDB database (ID: 6LSA). The PYMOL (Schrodinger version 2.4) tool was used to remove water molecules and examine the structure for prior attached ligands in the three-dimensional structure (Figure 9) and saved in the .pdb format

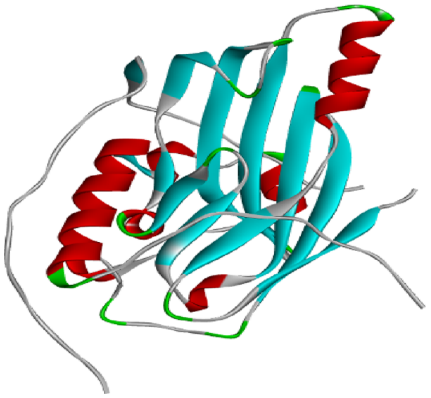

Figure 9. The three-dimensional structure of envelope glycoprotein (PDB ID: 6LS9).

for additional validation. The online GalaxyWEB tool (http://galaxy.seoklab.org/) was used for protein refinement and optimization, following which active sites were predicted with the use of the CASTp server online.[104]

Ligand Optimization. The chemical structures of potent LP phytochemicals were retrieved from the PubChem database (https://pubchem.ncbi. nlm.nih.gov/). Sdf-formatted files of luteolin, brassinolide, dolichin A, kievitone, and 2-hydroxygenistein (PubChem CID: 5280445, 115196, 44257432, 188458, and 5282074, respectively) were transformed into .pdb files using the OpenBabel l (v2.4.1) (https://sourceforge.net/projects/openbabel/files/openbabel/2.4.1/ (accessed on 18 June 2022))and ArgusLab software [V 4.6.0], adhering to the instructions in the ligand preparation.[105]

Protein Validation. The protein structure validation and evaluation of amino acid residues in the allowed and favored regions was performed using PROCHECK (https://www.ebi.ac.uk/thornton-srv/software/PROCHECK/) to obtain the Ramachandran plots. The protein selected for the present study, BHV-1 glycoprotein D (PDB ID: 6LSA), was found to be fit for molecular docking as they had a higher number of residues in the favored region.

Molecular Docking Interaction. The inhibition potential of the selected ligands was evaluated by performing molecular docking with the prepared protein using AutoDock Vina (v.1.2.0.).[106] To validate the addition of hydrogen molecules and add the necessary charge, the ligand(s) and protein .pdb formats were converted to .pdbqt formats. Thereafter, the active sites were identified and assigned and a grid box was created to cover the binding sites. The best possible models were picked out of the available poses and models, which had a range of binding affinities and RMSD values. Using the software Discovery Studio (v21.1.0.20298, Dassault Systèmes) [https://discover.3ds.com/discovery-studio-visualizer-

https://doi.org/10.1021/acsomega.3c01478
ACS Omega 2023, 8, 22684−22697

download (accessed on 18 June 2022)], interactions were visualized in the .pdb format. The binding residues were obtained to confirm the best docking poses.

Molecular Dynamics Simulations. The top protein and ligand combinations were chosen for molecular dynamics simulation using force field parameters from the CHARMM36 and CGenFF sets. The protein complexes were converted into .psf files, and trajectory files were obtained for further refinement. Cubic water boxes with transferable intermolecular potential and three-point water molecules were used to solvate the selected complexes, ensuring a safe distance of 10 Å between the protein target and the corners of the box. Short-range nonbonded interactions were computed with a 10 Å cutoff distance while long-range electrostatic associations were determined using the particle mesh Ewald method. The approximate results in an explicit solvent were obtained using the generalized born molecular mechanics surface area method. The simulation was carried out using NVT dynamics with a constant amount of substance, volume, and temperature. The temperature was set to 300 K, and the simulation was run for 100 ns with 1000 steps.

Conceptual DFT Studies. A conceptual DFT methodology was used for the determination of the Kohn−Sham (KS) method, and the lowest unoccupied and highest occupied molecular orbitals (LUMO and HOMO) and orbital, molecular, and electronic energies of the ligands were studied.[77−83,107−110] The molecular mechanics were calculated with the MMFF94 force field to determine the conformers of the studied ligands using the MarvinView 17.15 from ChemAxon.[111−114]

Following this, a preoptimization of the geometry and frequency calculation was achieved with the DFTB (Density Functional Tight Binding) methodology, with a further geometry re-optimization, frequency analysis, and calculation of the electronic properties and chemical reactivity descriptors achieved using the model chemistry based on the combination of the MN12SX density functional with the Def2TZVP basis set.[67,68,115] This determination was aided by the Gaussian 16 software and the SMD solvation model as it has been formerly evidenced to verify the "Koopmans in DFT" procedure[69−72,116] as means of corroboration of the nonappearance of imaginary frequencies to look for steadiness.

Computational Pharmacokinetics Analysis. The pharmacokinetics of ligands are important during new drug development/discovery, and hence, individual indices, i.e., Absorption, Distribution, Metabolism, Excretion, and Toxicity (ADMET) factors, were studied in silico using Chemicalize [https://chemicalize.com/].[117] Further information on the pharmacokinetic parameters was obtained using the canonical SMILES [https://biosig.unimelb.edu.au/pkcsm/] and other molecules with a similar structure to the studied ligands using Molinspiration software [https://www.molinspiration.com/] to predict the bioactivity ratings. Prediction of the most probable molecular protein target was performed using the SwissTargetPrediction [http://www.swisstargetprediction.ch/] webtool.[118]

Statistical Analysis. The results of experiments, executed in triplicate, were stated as mean ± SEM. To compare the differences between the *LP* extracts, LP-CuO NPs, and CuO NPs, the data were entered into the GraphPad Prism 8.0 software and subjected to one-way ANOVA followed by Tuckey's test. A *p*-value lower than 0.05 was regarded as significant.

AUTHOR INFORMATION

Corresponding Authors

Chandan Shivamallu − *Department of Biotechnology and Bioinformatics, JSS Academy of Higher Education and Research, Mysuru 570 015, India*; Email: chandans@jssuni.edu.in

Shashanka K. Prasad − *Department of Biotechnology and Bioinformatics, JSS Academy of Higher Education and Research, Mysuru 570 015, India; Plant Bioactive Compound Laboratory, Faculty of Agriculture, Chiang Mai University, Chiang Mai 50100, Thailand*; Email: shashankaprasad@jssuni.edu.in, shashanka.k@cmu.ac.th

Shiva Prasad Kollur − *School of Physical Sciences, Amrita Vishwa Vidyapeetham, Mysuru Campus, Mysuru, Karnataka 570 026, India*; orcid.org/0000-0003-3914-3933; Email: shivachemist@gmail.com

Authors

Smitha S. Bhat − *Department of Biotechnology and Bioinformatics, JSS Academy of Higher Education and Research, Mysuru 570 015, India*

Sushma Pradeep − *Department of Biotechnology and Bioinformatics, JSS Academy of Higher Education and Research, Mysuru 570 015, India*

Sharanagouda S. Patil − *ICAR-National Institute of Veterinary Epidemiology and Disease Informatics (NIVEDI), Bengaluru 560 064, India*

Norma Flores-Holguín − *Laboratorio Virtual NANOCOSMOS, Departamento de Medio Ambiente y Energía, Centro de Investigación en Materiales Avanzados, Chihuahua, Chihuahua 31136, Mexico*; orcid.org/0000-0002-4836-233X

Daniel Glossman-Mitnik − *Laboratorio Virtual NANOCOSMOS, Departamento de Medio Ambiente y Energía, Centro de Investigación en Materiales Avanzados, Chihuahua, Chihuahua 31136, Mexico*; orcid.org/0000-0002-9583-4256

Juan Frau − *Departament de Química, Facultat de Ciences, Universitat de les Illes Balears, E-07122 Palma de Mallorca, Spain*

Sarana Rose Sommano − *Plant Bioactive Compound Laboratory, Faculty of Agriculture, Chiang Mai University, Chiang Mai 50100, Thailand*

Nemat Ali − *Department of Pharmacology and Toxicology, College of Pharmacy, King Saud University, Riyadh 11451, Saudi Arabia*

Mohamed Mohany − *Department of Pharmacology and Toxicology, College of Pharmacy, King Saud University, Riyadh 11451, Saudi Arabia*

Complete contact information is available at: https://pubs.acs.org/10.1021/acsomega.3c01478

Author Contributions

#S.S.B. and S.P. are equal first authors. The manuscript was written through contributions of all authors.

Notes

The authors declare no competing financial interest.

ACKNOWLEDGMENTS

S.S.B., S.P., and C.S. acknowledge the leadership of JSS AHER for the support and infrastructure provided; S.S. acknowledges

https://doi.org/10.1021/acsomega.3c01478
ACS Omega 2023, 8, 22684−22697

the Faculty of Agriculture, CMU, for the support provided; S.K.P. acknowledges JSS AHER and the Faculty of Agriculture, CMU, for the support provided; S.S.P. acknowledges ICAR-NIVEDI for the infrastructure and support provided; D.G.-M. and N.F.-H. thank CIMAV for the support; J.F. thanks UIB for the support; N.A. and M.M. thank the infrastructure and funding provided by King Saud University; S.P.K. acknowledges the Director, Amrita Vishwa Vidyapeetham, Mysuru, for the support. This research was funded through the Researchers Supporting Project (RSPD2023R758), King Saud University, Riyadh, Saudi Arabia.

REFERENCES

(1) Turin, L.; Russo, S.; Poli, G. BHV-1: New Molecular Approaches to Control a Common and Widespread Infection. *Mol. Med.* **1999**, *5*, 261−284.
(2) Metzler, A. E.; Matile, H.; Gassmann, U.; Engels, M.; Wyler, R. European Isolates of Bovine Herpesvirus 1: A Comparison of Restriction Endonuclease Sites, Polypeptides, and Reactivity with Monoclonal Antibodies. *Arch. Virol.* **1985**, *85*, 57−69.
(3) Yates, W. D. A Review of Infectious Bovine Rhinotracheitis, Shipping Fever Pneumonia and Viral-Bacterial Synergism in Respiratory Disease of Cattle. *Can. J. Comp. Med.* **1982**, *46*, 225.
(4) Griffin, D. Economic Impact Associated with Respiratory Disease in Beef Cattle. *Vet. Clin. North Am. Food Anim. Pract.* **1997**, *13*, 367−377.
(5) Kapil, S.; Basaraba, R. J. Infectious Bovine Rhinotracheitis, Parainfluenza-3, and Respiratory Coronavirus. *Vet. Clin. North Am. Food Anim. Pract.* **1997**, *13*, 455−469.
(6) Edwards, A. Respiratory Diseases of Feedlot Cattle in Central USA. *Bov. Pract.* **1996**, *1996*, 5−7.
(7) Pourmahdi Borujeni, M.; Haji Hajikolaei, M. R.; Seifi Abad Shapouri, M. R.; Roshani, F. The Role of Sheep in the Epidemiology of Bovine Alphaherpesvirus 1 (BoHV-1). *Prev. Vet. Med.* **2020**, *174*, No. 104818.
(8) Lanave, G.; Larocca, V.; Losurdo, M.; Catella, C.; Capozza, P.; Tempesta, M.; Martella, V.; Buonavoglia, C.; Camero, M. Isolation and Characterization of Bovine Alphaherpesvirus 2 Strain from an Outbreak of Bovine Herpetic Mammillitis in a Dairy Farm. *BMC Vet. Res.* **2020**, *16*, 103.
(9) Kataria, R. S.; Tiwari, A. K.; Gupta, P. K.; Mehrotra, M. L.; Rai, A.; Bandyopadhyay, S. K. Detection of Bovine Herpesvirus 1 (BHV-1) Genomic Sequences in Bovine Semen Inoculated with BHV-1 by Polymerase Chain Reaction. *Acta Virol.* **1997**, *41*, 311−315.
(10) Verma, A.; Kumar, A. S.; Reddy, N.; Shinde, A. N. Sero-Prevalence of Infectious Bovine Rhinotracheitis in Dairy Animals with Reproductive Disorders in Uttar Pradesh, India. *Pakistan J. Biol. Sci.* **2014**, *17*, 720−724.
(11) Farooq, S.; Kumar, A.; Chaudhary, S.; Maan, S. Bovine Herpesvirus 1 (BoHV-1) in Cattle and Buffalo: A Review with Emphasis on Seroprevalence in India. *Int. J. Curr. Microbiol. Appl. Sci.* **2019**, *8*, 28−35.
(12) Nandi, S.; Kumar, M.; Manohar, M.; Chauhan, R. S. Bovine Herpes Virus Infections in Cattle. *Anim. Heal. Res. Rev.* **2009**, *10*, 85−98.
(13) Petrini, S.; Iscaro, C.; Righi, C. Antibody Responses to Bovine Alphaherpesvirus 1 (BoHV-1) in Passively Immunized Calves. *Viruses* **2019**, DOI: 10.3390/v11010023.
(14) Favier, P. A.; Marin, M. S.; Pérez, S. E. Role of Bovine Herpesvirus Type 5 (BoHV-5) in Diseases of Cattle. Recent Findings on BoHV-5 Association with Genital Disease. *Open Vet. J.* **2012**, *2*, 46−53.
(15) Rasheed, M. A.; Ansari, A. R.; Ihsan, A.; Navid, M. T.; ur-Rehman, S.; Raza, S. Prediction of Conserved Sites and Domains in Glycoproteins B, C and D of Herpes Viruses. *Microb. Pathog.* **2018**, *116*, 91−99.
(16) Domingo, E.; de Ávila, A. I.; Gallego, I.; Sheldon, J.; Perales, C. Viral Fitness: History and Relevance for Viral Pathogenesis and Antiviral Interventions. *Pathog. Dis.* **2019**, *77*, ftz021.
(17) Chou, S.; Lurain, N. S. *Antiviral Consideration for Transplantation Including Drug Resistance BT - Principles and Practice of Transplant Infectious Diseases*; Safdar, A., Ed.; Springer New York: New York, NY, 2019; pp. 953−975, DOI: 10.1007/978-1-4939-9034-4_54.
(18) Xu, J.; Li, X.; Jiang, B.; Feng, X.; Wu, J.; Cai, Y.; Zhang, X.; Huang, X.; Sealy, J. E.; Iqbal, M.; Li, Y. Antiviral Immunotoxin Against Bovine Herpesvirus-1: Targeted Inhibition of Viral Replication and Apoptosis of Infected Cell. *Front. Microbiol.* **2018**, DOI: 10.3389/fmicb.2018.00653.
(19) Fernandes, M. J. Screening of Brazilian Plants for Antiviral Activity against Animal Herpesviruses. *J. Med. Plants Res.* **2012**, *6*, DOI: 10.5897/JMPR10.040.
(20) Kaziyama, V. M.; Fernandes, M. J.; Simoni, I. Antiviral Activity of Commercially Available Medicinal Plants on Suid and Bovine Herpesviruses. *Rev. Bras. Plant. Med.* **2011**, *14*, 522−528.
(21) Dhierllate, F.; Fernandes, M. J.; Oliveira, R.; Pedro, C.; Carvalho, L.; Aline, O. In Vitro Cytotoxic and Anti-Herpesvirus Properties of Jackfruit (Artocarpus Heterophyllus Lam., Moraceae) Leaf Extracts. *J. Med. Plants Res.* **2020**, *14*, 225−231.
(22) Jennings, M. R.; Parks, R. J. Curcumin as an Antiviral Agent. *Viruses* **2020**, *12* (), DOI: 10.3390/v12111242.
(23) Ganjhu, R. K.; Mudgal, P. P.; Maity, H.; Dowarha, D.; Devadiga, S.; Nag, S.; Arunkumar, G. Herbal Plants and Plant Preparations as Remedial Approach for Viral Diseases. *Virusdisease* **2015**, *26*, 225−236.
(24) Kitazato, K.; Wang, Y.; Kobayashi, N. Viral Infectious Disease and Natural Products with Antiviral Activity. *Drug Discoveries Ther.* **2007**, *1*, 14−22.
(25) Adhikari, B.; Marasini, B. P.; Rayamajhee, B.; Bhattarai, B. R.; Lamichhane, G.; Khadayat, K.; Adhikari, A.; Khanal, S.; Parajuli, N. Potential Roles of Medicinal Plants for the Treatment of Viral Diseases Focusing on COVID-19: A Review. *Phyther. Res.* **2021**, *35*, 1298−1312.
(26) Wang, K.; Conlon, M.; Ren, W.; Chen, B. B.; Bączek, T. Natural Products as Targeted Modulators of the Immune System. *J. Immunol. Res.* **2018**.
(27) Khanna, K.; Kohli, S. K.; Kaur, R.; Bhardwaj, A.; Bhardwaj, V.; Ohri, P.; Sharma, A.; Ahmad, A.; Bhardwaj, R.; Ahmad, P. Herbal Immune-Boosters: Substantial Warriors of Pandemic Covid-19 Battle. *Phytomedicine* **2021**, *85*, No. 153361.
(28) Hou, T.; Xu, X. Recent Development and Application of Virtual Screening in Drug Discovery: An Overview. *Curr. Pharm. Des.* **2004**, *10*, 1011−1033.
(29) Zhong, F.; Xing, J.; Li, X.; Liu, X.; Fu, Z.; Xiong, Z.; Lu, D.; Wu, X.; Zhao, J.; Tan, X.; Li, F.; Luo, X.; Li, Z.; Chen, K.; Zheng, M.; Jiang, H. Artificial Intelligence in Drug Design. *Sci. China. Life Sci.* **2018**, *61*, 1191−1204.
(30) Niu, R.; Wang, Y.; Zhu, M.; Wen, Y.; Sun, J.; Shen, W.; Cheng, Y.; Zhang, J.; Jin, G.; Ma, H.; Hu, Z.; Shen, H.; Dai, J. Potentially Functional Polymorphisms in POU5F1 Gene Are Associated with the Risk of Lung Cancer in Han Chinese. *Biomed Res. Int.* **2015**, *2015*, No. 851320.
(31) Katsila, T.; Spyroulias, G. A.; Patrinos, G. P.; Matsoukas, M.-T. Computational Approaches in Target Identification and Drug Discovery. *Comput. Struct. Biotechnol. J.* **2016**, *14*, 177−184.
(32) Yu, W.; MacKerell, A. D. J. Computer-Aided Drug Design Methods. *Methods Mol. Biol.* **2017**, *1520*, 85−106.
(33) Chaturvedi, M.; Nagre, K.; Yadav, J. P. In Silico Approach for Identification of Natural Compounds as Potential COVID 19 Main Protease (M(pro)) Inhibitors. *Virusdisease* **2021**, *32*, 325−329.
(34) Kashyap, P.; Thakur, M.; Singh, N.; Shikha, D.; Kumar, S.; Baniwal, P.; Yadav, Y. S.; Sharma, M.; Sridhar, K.; Inbaraj, B. S. In Silico Evaluation of Natural Flavonoids as a Potential Inhibitor of Coronavirus Disease. *Molecules* **2022**, DOI: 10.3390/molecules27196374.

https://doi.org/10.1021/acsomega.3c01478
ACS Omega 2023, 8, 22684−22697

(35) Mousavi, S. S.; Karami, A.; Haghighi, T. M.; Tumilaar, S. G.; Fatimawali; Idroes, R.; Mahmud, S.; Celik, I.; Ağagündüz, D.; Tallei, T. E.; Emran, T. B.; Capasso, R. In Silico Evaluation of Iranian Medicinal Plant Phytoconstituents as Inhibitors against Main Protease and the Receptor-Binding Domain of SARS-CoV-2. *Molecules* **2021**, DOI: 10.3390/molecules26185724.
(36) Prasad, S. K.; Pradeep, S.; Shimavallu, C.; Kollur, S. P.; Syed, A.; Marraiki, N.; Egbuna, C.; Gaman, M.-A.; Kosakowska, O.; Cho, W. C.; Patrick-Iwuanyanwu, K. C.; Ortega Castro, J.; Frau, J.; Flores-Holguín, N.; Glossman-Mitnik, D. Evaluation of Annona Muricata Acetogenins as Potential Anti-SARS-CoV-2 Agents Through Computational Approaches. *Front. Chem.* **2020**, *8*, 1281.
(37) Mithilesh, S.; Raghunandan, D.; Suresh, P. K. In-Silico Identification of Natural Compounds from Traditional Medicine as Potential Drug Leads against SARS-CoV-2 Through Virtual Screening. *Proc. Natl. Acad. Sci., India, Sect. B* **2022**, *92*, 81−87.
(38) Bhattarai, B. R.; Adhikari, B.; Basnet, S.; Shrestha, A.; Marahatha, R.; Aryal, B.; Rayamajhee, B.; Poudel, P.; Parajuli, N. In Silico Elucidation of Potent Inhibitors from Natural Products for Nonstructural Proteins of Dengue Virus. *J. Chem.* **2022**, *2022*, 5398239.
(39) Mahmud, S.; Afrose, S.; Biswas, S.; Nagata, A.; Paul, G. K.; Mita, M. A.; Hasan, M. R.; Shimu, M. S. S.; Zaman, S.; Uddin, M. S.; Islam, M. S.; Saleh, M. A. Plant-Derived Compounds Effectively Inhibit the Main Protease of SARS-CoV-2: An in Silico Approach. *PLoS One* **2022**, *17*, No. e0273341.
(40) Singh, R.; Bhardwaj, V. K.; Sharma, J.; Purohit, R.; Kumar, S. In-Silico Evaluation of Bioactive Compounds from Tea as Potential SARS-CoV-2 Nonstructural Protein 16 Inhibitors. *J. Tradit. Complement. Med.* **2022**, *12*, 35−43.
(41) Mollica, A.; Costante, R.; Akdemir, A.; Carradori, S.; Stefanucci, A.; Macedonio, G.; Ceruso, M.; Supuran, C. T. Exploring New Probenecid-Based Carbonic Anhydrase Inhibitors: Synthesis, Biological Evaluation and Docking Studies. *Bioorg. Med. Chem.* **2015**, *23*, 5311−5318.
(42) Bhat, S. S.; Mahapatra, S. D.; R, S.; Sommano, S. R.; Prasad, S. K. Virtual Screening and Quantitative Structure–Activity Relationship of Moringa Oleifera with Melanoma Antigen A (MAGE-A) Genes against the Therapeutics of Non-Small Cell Lung Cancers (NSCLCs). *Cancers* **2022**, DOI: 10.3390/cancers14205052.
(43) Bhat, S. S.; Pradeep, S.; Jadhav, G.; Devegowda, D.; Sommano, S. R.; Shivamallu, C.; Kollur, S. P.; Prasad, S. K. In Silico Examination of Peptides Containing Selenium and Ebselen Backbone To Assess Their Tumoricidal Potential. *Int. J. Heal. Allied Sci.* **2022**, *11* (), DOI: 10.55691/2278-344X.1029.
(44) Shiragannavar, V. D.; Sannappa Gowda, N. G.; Puttahanumantharayappa, L. D.; Karunakara, S. H.; Bhat, S.; Prasad, S. K.; Kumar, D. P.; Santhekadur, P. K. The Ameliorating Effect of Withaferin A on High-Fat Diet-Induced Non-Alcoholic Fatty Liver Disease by Acting as an LXR/FXR Dual Receptor Activator. *Frontiers in Pharmacology* **2023**, DOI: 10.3389/fphar.2023.1135952.
(45) Bhat, S. S.; R, S.; Prasad, S. K. In Silico Screening of Violacein as an Epidermal Growth Factor Receptor Inhibitor. *Int. J. Heal. Allied Sci.* **2022**, *11*, 6. https://doi.org/https://rescon.jssuni.edu.in/ijhas/vol11/iss1/6
(46) Kurjogi, M. M.; Kaliwal, B. B. *In Silico* Identification and Characterization of Potential Drug Targets in Bovine Herpes Virus 4, Causing Bovine Mastitis. *Adv. Biol.* **2014**, *2014*, No. 369213.
(47) Naga Vamsi Krishna, A. Anti-Inflammatory and Anti-Diabetic Activities with Their Other Ethnomedicinal Properties of the Plants. *J. Med. Plants Stud.* **2013**, *1*, 87−96.
(48) Prasad, S. K.; Bhat, S. S.; Shivamallu, C.; Prasad, K. S. Biomedical Importance of Lablab Purpureus: A Review. *Med. Plants* **2022**, *14*, 20−29.
(49) S, P. Antibacterial Activity of the Volatile Oil of Lablab Purpureus Against Some Burn Isolates. *Int. J. Pharm. Sci. Res.* **2013**, *4* ().
(50) Saha, R. Antibacterial and Antioxidant Activities of a Food Lectin Isolated from the Seeds of Lablab Purpureous. *Am. J. Ethnomedicine* **2014**, *1*, 8−17.
(51) Thoyajakshi, R. S.; Poornima, D. Anticoagulant, Fibrinogenolytic and Anti-Platelet Aggregation Activities of Lablab Purpureus (L.) Sweet Seed Radicle Aqueous Extract. *Plant Sci. Today* **2021**, *8*, 89−94.
(52) Ahmed, M.; Shaha, S. R.; Dey, A.; Rahmatullah, M. AN INITIAL REPORT ON THE ANTIHYPERGLYCEMIC AND ANTINOCICEPTIVE POTENTIAL OF LABLAB PURPUREUS BEANS. *World J. Pharm. Pharm. Sci.* **2015**, *4*, 95−105.
(53) Bhaisare, M. Antioxidant Potential in Dolichose Lablab L. (Lablab Purpureus). *Indian J. Appl. Res.* **2019**, *9*, 35−36.
(54) Fakhoury, A. M.; Woloshuk, C. P. Inhibition of Growth of Aspergillus Flavus and Fungal Alpha-Amylases by a Lectin-like Protein from Lablab Purpureus. *Mol. Plant-Microbe Interact.* **2001**, *14*, 955−961.
(55) Rahman, S. A.; Akhter, M. S. Antibacterial and Cytotoxic Activity of Seeds of White Hyacinth Bean (*Lablab Purpureus* L. Sweet "White").". *J. Adv. Biotechnol. Exp. Ther.* **2018**, *1*, 49−54.
(56) Pramod, C.; Nair, S. IN-VITRO ANALYSIS OF GENISTEIN ISOLATED FROM LABLAB PURPUREUS LINN INHIBITED ON LPS INDUCED INFLAMMATION IN HPBMCS CELLS VIA A TLR MEDIATED NF-KB PATH WAY AND OXIDATIVE STRESS CONDITION. *WORLD J. Pharm. Pharm. Sci.* **2021**, *9*, 1326−1340.
(57) Siphali, S.; Dwaraka, D.; Amonsou, E.; Mellem, J. In Vitro Antioxidant and Apoptotic Activity of Lablab Purpureus (L.) Sweet Isolate and Hydrolysates. *Food Sci. Technol.* **2021**, *2061*, 1−9.
(58) RufusAuxilia, L.; Mowna Sundari, T. Molecular Docking Studies of Dolichin A and B, Pterocarpans from Horsegram (Macrotyloma Uniflorum) against HIV Replication Enzymes. *Int. J. Comput. Appl.* **2013**, *75*, 19−23.
(59) Ye, X. Y.; Wang, H. X.; Ng, T. B. Dolichin, a New Chitinase-like Antifungal Protein Isolated from Field Beans (Dolichos Lablab). *Biochem. Biophys. Res. Commun.* **2000**, *269*, 155−159.
(60) Yan, H.; Ma, L.; Wang, H.; Wu, S.; Huang, H.; Gu, Z.; Jiang, J.; Li, Y. Luteolin Decreases the Yield of Influenza A Virus in Vitro by Interfering with the Coat Protein I Complex Expression. *J. Nat. Med.* **2019**, *73*, 487−496.
(61) Animashaun, T.; Mahmood, N. Inhibitory Effects of Novel Mannose-Binding Lectins on HIV-Infectivity and Syncytium Formation. *Antiviral Chem. Chemother.* **1993**, *4*, 145−153.
(62) Jazie, A. A.; Albaaji, A. J.; Abed, S. A. A Review on Recent Trends of Antiviral Nanoparticles and Airborne Filters: Special Insight on COVID-19 Virus. *Air Qual. Atmos. Heal.* **2021**, *14*, 1811−1824.
(63) Kobayashi, K.; Wei, J.; Iida, R.; Ijiro, K.; Niikura, K. Surface Engineering of Nanoparticles for Therapeutic Applications. *Polym. J.* **2014**, *46*, 460−468.
(64) Gurunathan, S.; Qasim, M.; Choi, Y.; Do, J. T.; Park, C.; Hong, K.; Kim, J.-H.; Song, H. Antiviral Potential of Nanoparticles—Can Nanoparticles Fight Against Coronaviruses? *Nanomaterials* **2020**, DOI: 10.3390/nano10091645.
(65) Shamaila, S.; Sajjad, A. K. L.; Ryma, N.-A.; Farooqi, S. A.; Jabeen, N.; Majeed, S.; Farooq, I. Advancements in Nanoparticle Fabrication by Hazard Free Eco-Friendly Green Routes. *Appl. Mater. Today* **2016**, *5*, 150−199.
(66) Zeedan, G.; El-Razik, K.; Allam, A.; Abdelhamed, A.; Abou-Zeina, H. Evaluations of Potential Antiviral Effects of Green Zinc Oxide and Silver Nanoparticles against Bovine Herpesvirus-1. *Adv. Anim. Vet. Sci.* **2020**, *8*, 433−443.
(67) Weigend, F.; Ahlrichs, R. Balanced Basis Sets of Split Valence, Triple Zeta Valence and Quadruple Zeta Valence Quality for H to Rn: Design and Assessment of Accuracy. *Phys. Chem. Chem. Phys.* **2005**, *7*, 3297−3305.
(68) Weigend, F. Accurate Coulomb-Fitting Basis Sets for H to Rn. *Phys. Chem. Chem. Phys.* **2006**, *8*, 1057−1065.
(69) Flores-Holguín, N.; Frau, J.; Glossman-Mitnik, D. Conceptual DFT-Based Computational Peptidology of Marine Natural Compounds: Discodermins A−H. *Molecules* **2020**, DOI: 10.3390/molecules25184158.

https://doi.org/10.1021/acsomega.3c01478
ACS Omega 2023, 8, 22684−22697

(70) Marenich, A. V.; Cramer, C. J.; Truhlar, D. G. Universal Solvation Model Based on Solute Electron Density and on a Continuum Model of the Solvent Defined by the Bulk Dielectric Constant and Atomic Surface Tensions. *J. Phys. Chem. B* **2009**, *113*, 6378−6396.
(71) Flores, N.; Frau, J.; Glossman-Mitnik, D. *Conceptual DFT as a Helpful Chemoinformatics Tool for the Study of the Clavanin Family of Antimicrobial Marine Peptides*; 2019, DOI: 10.5772/intechopen.88657.
(72) Flores-Holguín, N.; Frau, J.; Glossman-Mitnik, D. Virtual Screening of Marine Natural Compounds by Means of Chemoinformatics and CDFT-Based Computational Peptidology. *Mar. Drugs* **2020**, *18*, 479.
(73) Domingo, L. R.; Ríos-Gutiérrez, M.; Pérez, P. Applications of the Conceptual Density Functional Theory Indices to Organic Chemistry Reactivity. *Molecules* **2016**, *21*, 748.
(74) Domingo, L. R.; Aurell, M. J.; Pérez, P.; Contreras, R. Quantitative Characterization of the Global Electrophilicity Power of Common Diene/Dienophile Pairs in Diels−Alder Reactions. *Tetrahedron* **2002**, *58*, 4417−4423.
(75) Domingo, L. R.; Sáez, J. A. Understanding the Mechanism of Polar Diels−Alder Reactions. *Org. Biomol. Chem.* **2009**, *7*, 3576−3583.
(76) Pérez, P.; Domingo, L. R.; José Aurell, M.; Contreras, R. Quantitative Characterization of the Global Electrophilicity Pattern of Some Reagents Involved in 1,3-Dipolar Cycloaddition Reactions. *Tetrahedron* **2003**, *59*, 3117−3125.
(77) Jensen, F. *Introduction to Computational Chemistry*, 2nd ed.; John Wiley & Sons: Chichester, 2007.
(78) Cramer, C. *Essentials of Computational Chemistry - Theories and Models*; John Wiley & Sons: Chichester, 2004.
(79) Parr, R.; Yang, W. *Density-Functional Theory of Atoms and Molecules*; Oxford University Press: New York, NY, 1989.
(80) Chermette, H. Chemical Reactivity Indexes in Density Functional Theory. *J. Comput. Chem.* **1999**, *20*, 129−154.
(81) Geerlings, P.; De Proft, F.; Langenaeker, W. Conceptual Density Functional Theory. *Chem. Rev.* **2003**, *103*, 1793−1874.
(82) Geerlings, P.; Chamorro, E.; Chattaraj, P. K.; De Proft, F.; Gázquez, J. L.; Liu, S.; Morell, C.; Toro-Labbé, A.; Vela, A.; Ayers, P. Conceptual Density Functional Theory: Status, Prospects, Issues. *Theor. Chem. Acc.* **2020**, *139*, 36.
(83) Geerlings, P.; Proft, F.; Ayers, P. Theoretical Aspects of Chemical Reactivity. In *Chemical reactivity and the shape function*; 2007; pp. 1−17.
(84) Morell, C.; Grand, A.; Toro-Labbé, A. New Dual Descriptor for Chemical Reactivity. *J. Phys. Chem. A* **2005**, *109*, 205−212.
(85) Martínez-Araya, J. I. Explaining Reaction Mechanisms Using the Dual Descriptor: A Complementary Tool to the Molecular Electrostatic Potential. *J. Mol. Model.* **2013**, *19*, 2715−2722.
(86) Martínez-Araya, J. I. Revisiting Caffeate's Capabilities as a Complexation Agent to Silver Cation in Mining Processes by Means of the Dual Descriptor–a Conceptual DFT Approach. *J. Mol. Model.* **2012**, *18*, 4299−4307.
(87) Dubey, N. K.; Kumar, R.; Tripathi, P. Global Promotion of Herbal Medicine: India's Opportunity. *Curr. Sci.* **2004**, *86*, 37−41.
(88) Goel, A.; Singh, R.; Dash, S.; Gupta, D.; Pillai, A.; Yadav, S.; Bhatia, A. Antiviral Activity of Few Selected Indigenous Plants Against Bovine Herpes Virus-1. *J. Immunol. Immunopathol.* **2011**, *13*, 30−37.
(89) Fukuchi, K.; Sakagami, H.; Okuda, T.; Hatano, T.; Tanuma, S.; Kitajima, K.; Inoue, Y.; Inoue, S.; Ichikawa, S.; Nonoyama, M.; Konno, K. Inhibition of Herpes Simplex Virus Infection by Tannins and Related Compounds. *Antiviral Res.* **1989**, *11*, 285−297.
(90) Ono, K.; Nakane, H.; Fukushima, M.; Chermann, J. C.; Barré-Sinoussi, F. Inhibition of Reverse Transcriptase Activity by a Flavonoid Compound, 5,6,7-Trihydroxyflavone. *Biochem. Biophys. Res. Commun.* **1989**, *160*, 982−987.
(91) Chang, L.; Zhu, L. Dewormer Drug Fenbendazole Has Antiviral Effects on BoHV-1 Productive Infection in Cell Cultures. *J. Vet. Sci.* **2020**, *21*, No. e72.
(92) Fiorito, F.; Cerracchio, C.; Salvatore, M. M.; Serra, F.; Pucciarelli, A.; Amoroso, M. G.; Nicoletti, R.; Andolfi, A. Antiviral Property of the Fungal Metabolite 3-O-Methylfunicone in Bovine Herpesvirus 1 Infection. *Microorganisms* **2022**, *10*, 188.
(93) Felipe, A. M. M.; Rincão, V. P.; Benati, F. J.; Linhares, R. E. C.; Galina, K. J.; de Toledo, C. E. M.; Lopes, G. C.; de Mello, J. C. P.; Nozawa, C. Antiviral Effect of Guazuma Ulmifolia and Stryphnodendron Adstringens on Poliovirus and Bovine Herpesvirus. *Biol. Pharm. Bull.* **2006**, *29*, 1092−1095.
(94) Fayaz, A. M.; Ao, Z.; Girilal, M.; Chen, L.; Xiao, X.; Kalaichelvan, P. T.; Yao, X. Inactivation of Microbial Infectiousness by Silver Nanoparticles-Coated Condom: A New Approach to Inhibit HIV-and HSV-Transmitted Infection. *Int. J. Nanomed.* **2012**, *7*, 5007.
(95) Xiang, D.; Chen, Q.; Pang, L.; Zheng, C. Inhibitory Effects of Silver Nanoparticles on H1N1 Influenza A Virus in Vitro. *J. Virol. Methods* **2011**, *178*, 137−142.
(96) Turnlund, J. R. Human Whole-Body Copper Metabolism. *Am. J. Clin. Nutr.* **1998**, *67*, 960S−964S.
(97) Bilian, X. Intrauterine Devices. *Best Pract. Res. Clin. Obstet. Gynaecol.* **2002**, *16*, 155−168.
(98) Jones, C. Herpes Simplex Virus Type 1 and Bovine Herpesvirus 1 Latency. *Clin. Microbiol. Rev.* **2003**, *16*, 79−95.
(99) Alves Dummer, L.; Pereira Leivas Leite, F.; van Drunen Littel-van den Hurk, S. Bovine Herpesvirus Glycoprotein D: A Review of Its Structural Characteristics and Applications in Vaccinology. *Vet. Res.* **2014**, *45*, 111.
(100) Prasad, S.; Veeresh, P.; Ramesh, P.; Natraj, S.; Madhunapantula, S.; Devegowda, D. Phytochemical Fractions from *Annona Muricata* Seeds and Fruit Pulp Inhibited the Growth of Breast Cancer Cells through Cell Cycle Arrest at G_0/G_1 Phase. *J. Cancer Res. Ther.* **2020**, *16*, 1235−1249.
(101) Rangel, W. M.; Boca Santa, R. A. A.; Riella, H. G. A Facile Method for Synthesis of Nanostructured Copper (II) Oxide by Coprecipitation. *J. Mater. Res. Technol.* **2020**, *9*, 994−1004.
(102) Ansari, M.; Sharififar, F.; Arabzadeh, A. M.; Mehni, F.; Mirtadzadini, M.; Iranmanesh, Z.; Nikpour, N. In Vitro Evaluation of Anti-Herpes Simplex-1 Activity of Three Standardized Medicinal Plants from Lamiaceae. *Anc. Sci. Life* **2014**, *34*, 33−38.
(103) Feoktistova, M.; Geserick, P.; Leverkus, M. Crystal Violet Assay for Determining Viability of Cultured Cells. *Cold Spring Harb. Protoc.* **2016**, *2016*, pdb.prot087379.
(104) Tian, W.; Chen, C.; Lei, X.; Zhao, J.; Liang, J. CASTp 3.0: Computed Atlas of Surface Topography of Proteins. *Nucleic Acids Res.* **2018**, *46*, W363−W367.
(105) O'Boyle, N. M.; Banck, M.; James, C. A.; Morley, C.; Vandermeersch, T.; Hutchison, G. R. Open Babel: An Open Chemical Toolbox. *Aust. J. Chem.* **2011**, *3*, 33.
(106) Eberhardt, J.; Santos-Martins, D.; Tillack, A. F.; Forli, S. AutoDock Vina 1.2.0: New Docking Methods, Expanded Force Field, and Python Bindings. *J. Chem. Inf. Model.* **2021**, *61*, 3891−3898.
(107) Chakraborty, D.; Chattaraj, P. K. Conceptual Density Functional Theory Based Electronic Structure Principles. *Chem. Sci.* **2021**, *12*, 6264−6279.
(108) E. G., Lewars *Computational Chemistry Introduction to the Theory and Applications of Molecular and Quantum Mechanics*; Kluwer Academic Publishers: Dordrecht, 2011.
(109) Young, D. *Computational Chemistry: A Practical Guide for Applying Techniques to Real World Problems*; John Wiley & Sons: New York, NY, 2001.
(110) Chattaraj, P. K. *Chemical Reactivity Theory*, 1st ed.; CRC press: Boca Raton, 2009, DOI: 10.1201/9781420065442.
(111) Halgren, T. A. Merck Molecular Force Field. II. MMFF94 van Der Waals and Electrostatic Parameters for Intermolecular Interactions. *J. Comput. Chem.* **1996**, *17*, 520−552.
(112) Halgren, T. A. Merck Molecular Force Field. I. Basis, Form, Scope, Parameterization, and Performance of MMFF94. *J. Comput. Chem.* **1996**, *17*, 490−519.

https://doi.org/10.1021/acsomega.3c01478
ACS Omega 2023, 8, 22684−22697

(113) Halgren, T. A. Merck Molecular Force Field. V. Extension of MMFF94 Using Experimental Data, Additional Computational Data, and Empirical Rules. *J. Comput. Chem.* **1996**, *17*, 616−641.
(114) Halgren, T. A.; Nachbar, R. B. Merck Molecular Force Field. IV. Conformational Energies and Geometries for MMFF94. *J. Comput. Chem.* **1996**, *17*, 587−615.
(115) Peverati, R.; Truhlar, D. G. Screened-Exchange Density Functionals with Broad Accuracy for Chemistry and Solid-State Physics. *Phys. Chem. Chem. Phys.* **2012**, *14*, 16187−16191.
(116) Flores, N.; Frau, J.; Glossman-Mitnik, D. A Fast and Simple Evaluation of the Chemical Reactivity Properties of the Pristinamycin Family of Antimicrobial Peptides. *Chem. Phys. Lett.* **2019**, *739*, No. 137021.
(117) Daina, A.; Michielin, O.; Zoete, V. SwissADME: A Free Web Tool to Evaluate Pharmacokinetics, Drug-Likeness and Medicinal Chemistry Friendliness of Small Molecules. *Sci. Rep.* **2017**, *7*, 1−13.
(118) Daina, A.; Michielin, O.; Zoete, V. SwissTargetPrediction: Updated Data and New Features for Efficient Prediction of Protein Targets of Small Molecules. *Nucleic Acids Res.* **2019**, *47*, W357−W364.

https://doi.org/10.1021/acsomega.3c01478
ACS Omega 2023, 8, 22684−22697